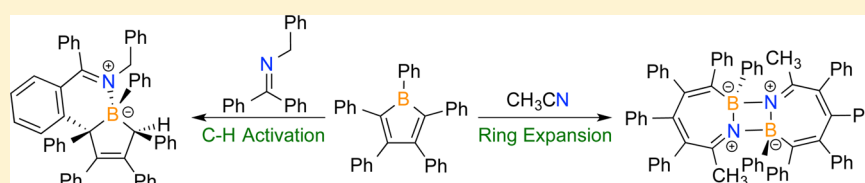


Reactions of Imines, Nitriles, and Isocyanides with Pentaphenylborole: Coordination, Ring Expansion, C–H Bond Activation, and Hydrogen Migration Reactions

Kexuan Huang,[†] Shannon A. Couchman,[‡] David J. D. Wilson,[‡] Jason L. Dutton,[‡] and Caleb D. Martin^{*,†}[†]Department of Chemistry and Biochemistry, Baylor University, One Bear Place #97348, Waco, Texas 76798, United States[‡]Department of Chemistry and Physics, La Trobe Institute for Molecular Science, La Trobe University, Melbourne, Victoria, Australia, 3086

S Supporting Information



ABSTRACT: The reactions of pentaphenylborole with imines, isocyanides, and acetonitrile were investigated experimentally and theoretically. On the basis of literature precedent, we envisioned that the dipolar substrates would undergo facile ring expansion reactions to yield new BNC₅ heterocycles. For acetonitrile and one particular imine, this ring expansion process was observed. However, in many cases, unexpected reactivity occurred. This included hydride migration of an imine ring expanded product and the *ortho* C–H bond activation of an aryl group of an imine if two phenyl groups were present on the α -carbon. A bulky group on the nitrogen atom of an imine prevented coordination to the boron center, and no reaction was observed, indicating that coordination to the borole is a critical step for any type of reaction to occur. Isocyanides made coordination complexes, but heating to induce further reactivity resulted in mixtures. The mechanisms were elucidated via DFT calculations, which complement the experimental findings.

■ INTRODUCTION

Boroles are very reactive heterocycles attributed to their antiaromatic nature deriving from the four π -electrons in the planar BC₄ core.^{1–4} The electron deficiency in boroles permits facile one- and two-electron reductions to form the non-aromatic radical anion and aromatic dianion, respectively.^{5–13} The butadiene backbone is susceptible to Diels–Alder chemistry, engaging in [4+2] cycloaddition reactions with dienophile partners.^{14–17} These species also react with dihydrogen and Si–H bonds to produce boracycles with H or Si introduced at the 2- and 5-positions of the borole, making the carbon centers adjacent to boron saturated.^{18–21} The driving force in these reactions is the alleviation of the unfavorable antiaromatic arrangement in the borole heterocycle.

The coordination of Lewis bases to the boron center also relieves the borole from its antiaromaticity by occupying boron's empty p-orbital and disrupting the extended conjugation in the ring.^{10,11,22–30} Surprisingly, several of these adducts can engage in further reactivity, typically resulting in a ring expansion reaction if an electrophilic site is present on the Lewis basic moiety. This has been observed in reactions with carbon monoxide, alkynes, azides, and isocyanides, as well as with a ketone and an aldehyde (Figure 1, 4–12).^{17,29,31–35} These ring expansion products are interesting, as unsaturated boron heterocycles have attractive electronic properties and are

challenging synthetic targets.^{36–47} With the exception of carbon monoxide, the ring expansion occurs rapidly and the coordination complex is not observed, but implied by the reaction products or theoretical calculations. The coordination, then ring expansion protocol appears to be an effective route to generate new boracycles; however the versatility and the mechanism have not been well developed.

In light of the lack of experimental data on the adduct intermediates of these compounds, we envisioned that carbon–nitrogen systems such as imines, nitriles, and isocyanides could provide further insight into this chemistry and also generate new boracycles. These systems are good Lewis bases, but still possess a 1,2-dipole that is effective for a 1,2-insertion to a seven-membered heterocycle to occur (cf. 7–9).³³ The ring-expanded products would be B–N-containing hybrid organic/inorganic heterocycles, compounds that have gained significant interest in recent years for their useful biological activity as well as photophysical and electrochemical properties.^{48,49} In most cases, the desired adduct was stable, isolated, and characterized. The subsequent ring expansion could be induced by prolonged reaction times or thermolysis for some substrates. However, this route proved not to be universal and has led to some unusual reactivity including hydrogen migration and aryl C–H

Received: May 12, 2015

Published: September 1, 2015



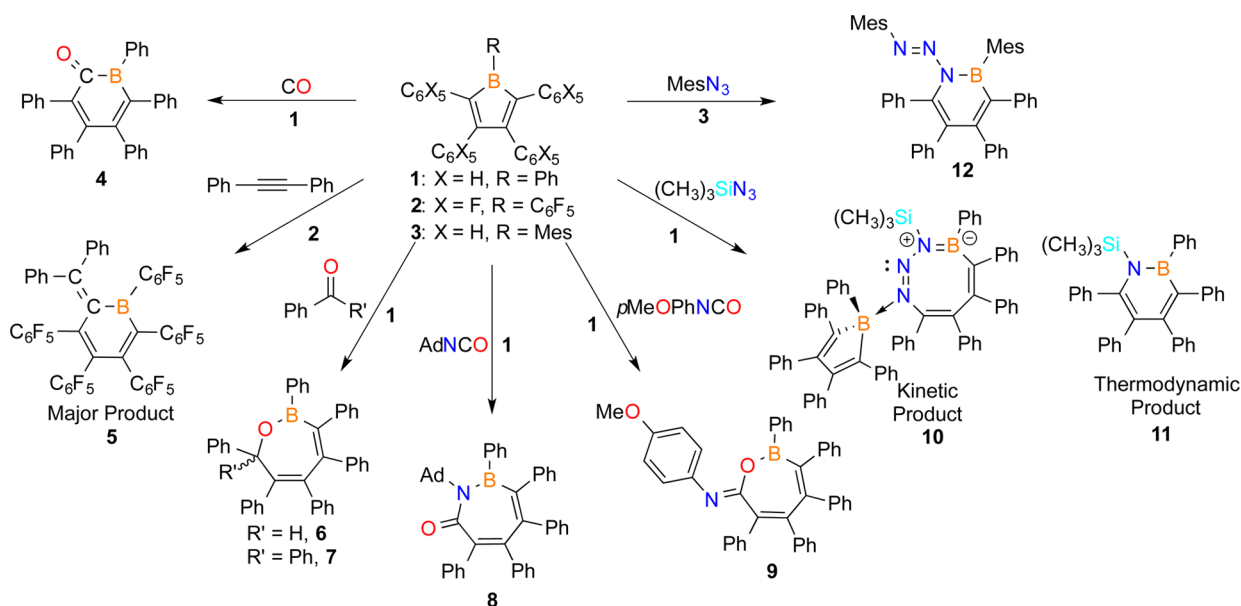


Figure 1. Ring expansion reactivity of boroles proceeding via an adduct intermediate.

bond activation reactions. An in-depth computational study provided significant insight into the reaction mechanisms.

RESULTS AND DISCUSSION

We first focused our attention on imines due to their resemblance to the recently studied isocyanates. Both 1-adamantyl- and *para*-methoxyphenyl-isocyanate reacted with pentaphenylborole (**1**) by the insertion of a 1,2-dipole into the ring.³³ The 1-adamantyl derivative inserted a C–N unit into the BC₄ ring (**8**), whereas the *para*-methoxyphenyl variant inserted a C–O unit (**9**) due to the differing nucleophilic sites of the isocyanate. The chemistry should be simplified for imines by only having the C=N functionality. It is also noteworthy that well-defined boron/imine coordination complexes have been reported, giving the potential to isolate the borole-imine adduct intermediates prior to a ring expansion.⁵⁰ We examined the reactions of pentaphenylborole **1** with imines **13**–**15**, which feature a phenyl group on carbon and variable groups as the other substituent on carbon and nitrogen (Figure 2).

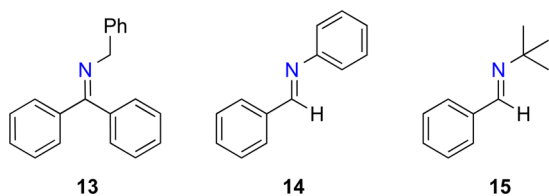


Figure 2. Imines of focus in this study.

Adding a CH₂Cl₂ solution of imine **13** (featuring two phenyl groups on the α -carbon and a benzyl group on nitrogen) to the dark blue borole solution in the same solvent resulted in an immediate color change to a red solution (Scheme 1). Removing the solvent *in vacuo*, redissolving the solids in CDCl₃, and acquiring a ¹¹B{¹H} NMR spectrum revealed a single resonance shifted significantly upfield in comparison to the free borole **1**, consistent with the complete conversion to a four-coordinate boron species ($\delta = 6.0$ cf. **1**, $\delta = 65.0$). Crystals suitable for an X-ray diffraction study were grown from a

CH₂Cl₂ solution via vapor diffusion into hexanes, confirming the identity as the expected coordination complex **16** (Figure 3a).

We postulated that the imine-borole adduct **16** could easily be converted into the ring-expanded BNC₅ heterocyclic species due to the proximity of the electrophilic α -carbon of the imine and the nucleophilic endocyclic B–C bond. Heating a toluene solution of **16** at 80 °C for 24 h resulted in a color change from red to a yellow solution. Removing the volatiles *in vacuo* afforded a pale yellow solid. The ¹¹B{¹H} NMR spectrum of the redissolved solids in CDCl₃ revealed a peak in almost the same position as the adduct, indicating the retention of a four-coordinate boron center ($\delta = 4.7$ cf. **16** $\delta = 6.0$). In addition to the expected aryl protons, three other resonances were observed, each as a broad peak at 6.39, 5.02, and 4.32 ppm integrating in a 1:1:1 ratio. These were very different than the methylene protons of the benzyl group of adduct **16**, which appeared as a broad peak at 5.32 ppm with an integration equal to two with respect to the 40 aryl protons. Crystals grown from a CH₂Cl₂ solution via vapor diffusion into hexanes permitted an X-ray diffraction study identifying the compound as the product resulting from the 2,5-addition of the *ortho* C–H bond from one of the phenyl rings of ketimine **13** into the borole (**17**, Figure 3b). The groups of Piers and Braunschweig have shown that free boroles undergo such 2,5-addition reactions with H₂ and HSiEt₃.^{18,20} The carbon and hydrogen atoms from the phenyl group were introduced on the carbon atoms adjacent to boron in a *syn* configuration. The C=N and B–N distances of the C–H activated product **17** and the coordination complex **16** are virtually identical [1.299(3) and 1.620(3) Å; cf. 1.303(3) and 1.637(3) Å, respectively]. One enantiomer [C(1)-S, C(4)-R, B-R] was found in the asymmetric unit, but the other enantiomer was also present in a 1:1 ratio due to the center of symmetry associated with the *P* $\bar{1}$ space group. Interestingly, no other diastereomers were observed in the ¹H NMR spectrum of the crude product. On the basis of the solid-state structure, we assigned the three broad peaks in the ¹H NMR spectrum as the two asymmetric benzyl protons (due to the bulky groups) and the third peak from the proton introduced on the carbon adjacent to boron in the boracycle.

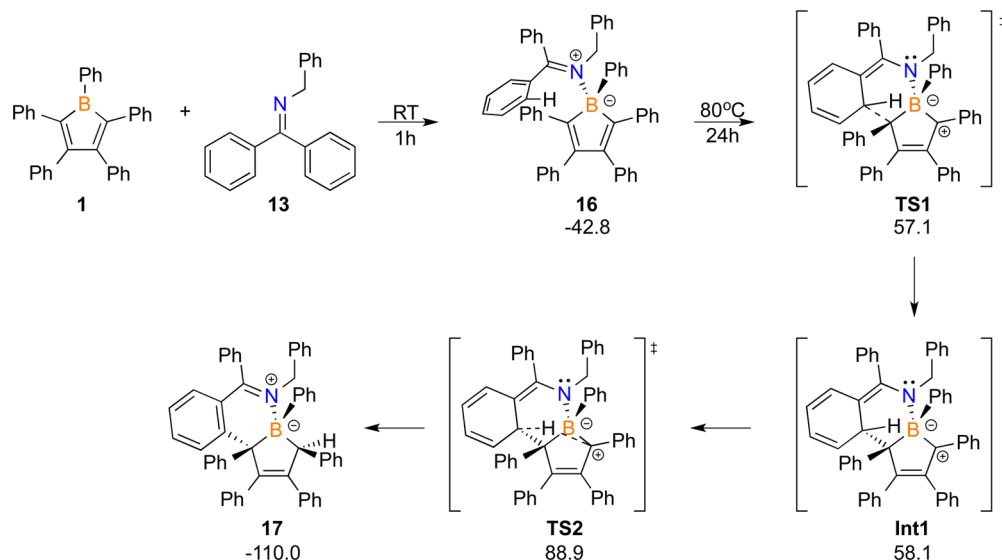
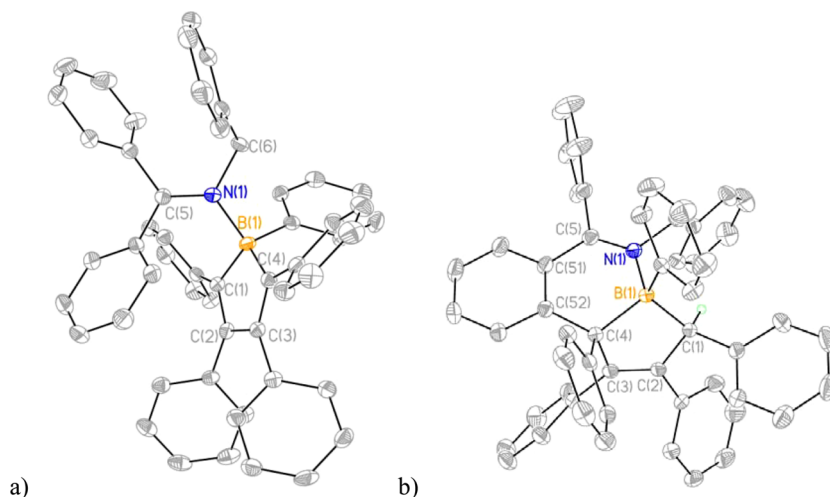
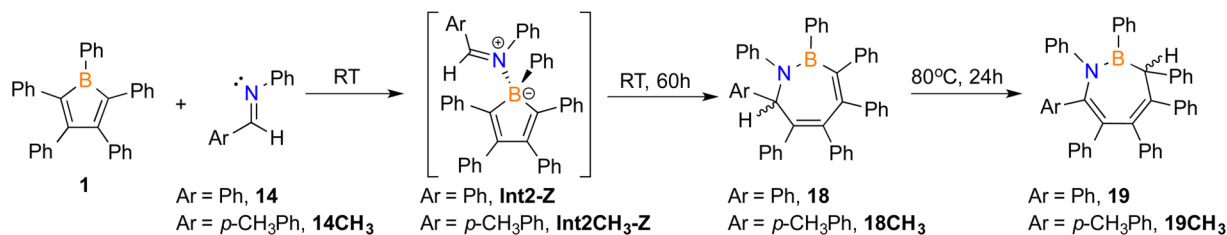
Scheme 1. Coordination and Thermally Induced C–H Bond Activation of Imine 13^a^aReaction energies (ΔG) are in kJ/mol relative to **1** and **13**.

Figure 3. Solid-state structures of **16** (a) and **17** (b). Hydrogen atoms are omitted (except on the quaternary carbon of **17**) for clarity, and ellipsoids are drawn at the 50% probability level. Selected bond lengths (Å) and angles (deg) for **16**: B(1)–N(1) 1.637(3), B(1)–C(1) 1.630(3), B(1)–C(4) 1.625(3), N(1)–C(5) 1.303(3), N(1)–C(6) 1.495(3), C(1)–C(2) 1.363(3), C(2)–C(3) 1.494(3), C(3)–C(4) 1.364(3), N(1)–B(1)–C(1) 114.17(17), C(5)–N(1)–B(1) 124.28(17), C(5)–N(1)–C(6) 119.16(17); for **17**: B(1)–N(1) 1.620(3), B(1)–C(1) 1.670(3), B(1)–C(4) 1.680(3), N(1)–C(5) 1.299(3), N(1)–C(6) 1.481(3), C(1)–C(2) 1.514(3), C(2)–C(3) 1.342(3), C(3)–C(4) 1.541(3), N(1)–B(1)–C(1) 104.84(18), C(5)–N(1)–B(1) 126.23(19).

Scheme 2. Ring Expansion and Hydrogen Migration Reaction of Borole **1** with Imines **14** and **14CH₃**

Density functional theory calculations indicate that the formation of the C–H activated product is thermodynamically favorable, with **17** lying 67.2 kJ/mol lower in energy than adduct **16** on the potential energy surface (Scheme 1). The calculations suggest that the reaction proceeds via the

butadiene moiety of the borole attacking the *ortho* carbon of one of the aryl groups on the imine, resulting in the dearomatization of the aryl group facilitated by the imine (TS1). The potential energy surface is very flat around TS1 and Int1; however both are distinct species that are readily

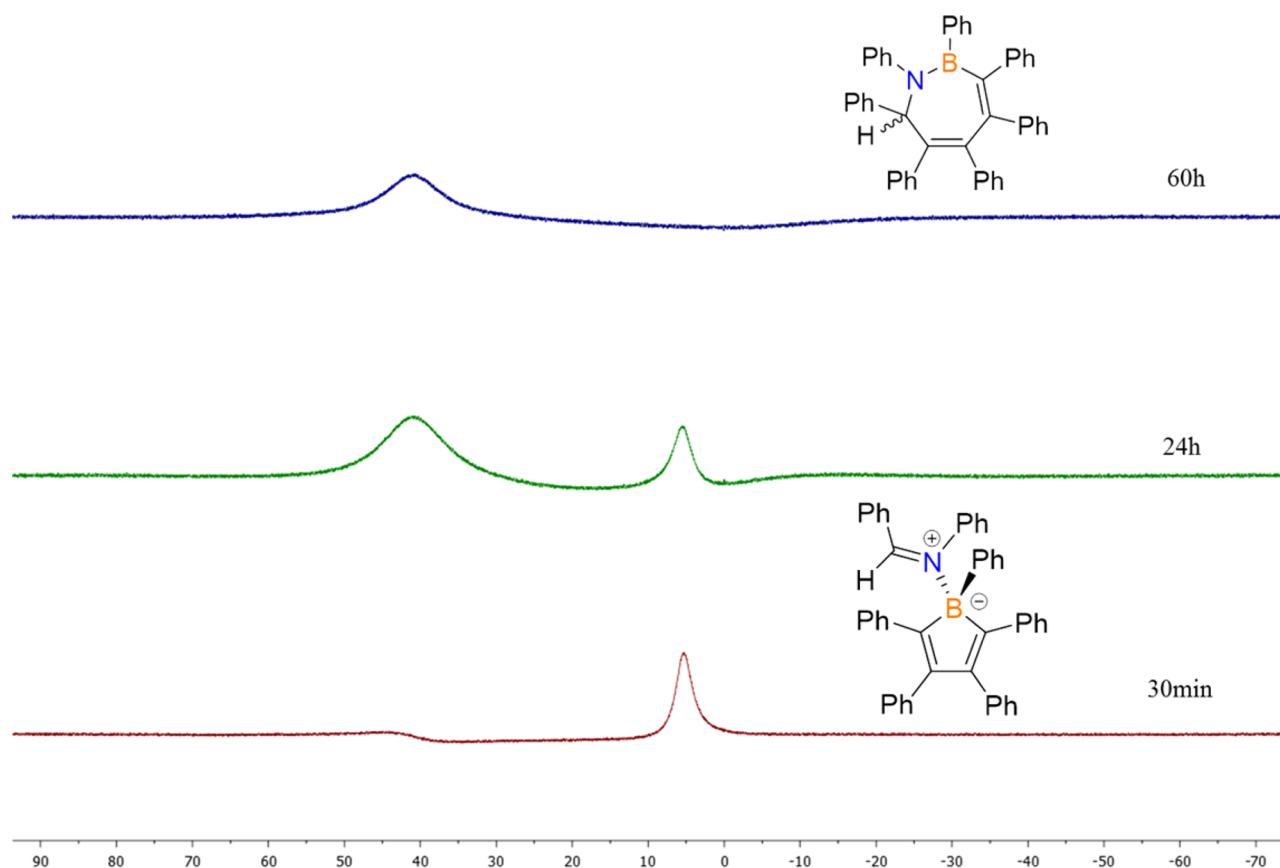


Figure 4. Stacked $^{11}\text{B}\{^1\text{H}\}$ NMR plot displaying the reaction of borole **1** with imine **14** at room temperature in CDCl_3 .

optimized.⁵¹ The hydride migrates to the carbocation on the same face of the boracycle (**TS2**), justifying the *syn* configuration observed and also the absence of multiple diastereomers. This process also allows the rearomatization of the phenyl ring, once again assisted by the nitrogen center. Erker recently reported the synthesis of an *N*-phenyl amino-substituted borole, which undergoes an intramolecular aromatic C–H addition reaction.⁵² However, a 2,5-addition reaction from the Lewis basic moiety of a borole adduct has not been reported.

We then turned our attention to aldimine **14**, featuring a hydrogen on the α -carbon and a phenyl group on nitrogen, to determine if reducing the bulk at the carbon center would alter the reaction outcome. The 1:1 reaction of **14** with borole **1** in CH_2Cl_2 at room temperature resulted in the same color change from deep blue to deep red over a period of 5 min (**Scheme 2**). The $^{11}\text{B}\{^1\text{H}\}$ NMR spectrum showed a resonance at $\delta = 5.5$, consistent with the formation of the four-coordinate adduct. The adduct could not be isolated since it immediately began converting to a new species, observed as a broad resonance in the $^{11}\text{B}\{^1\text{H}\}$ NMR spectrum at 41.8 ppm, indicative of a three-coordinate boron species. After stirring the solution for 60 h, the color had turned from red to colorless and the $^{11}\text{B}\{^1\text{H}\}$ NMR spectrum indicated complete conversion to the three-coordinate species (**Figure 4**).

Monitoring the reaction by ^1H NMR spectroscopy was informative due to the diagnostic proton on the α -carbon of imine **14** (**Figure 5**). Acquiring a spectrum after 30 min showed three singlets indicative of three different imine-containing species. The free imine was observed in addition to a major species with the resonance shifted downfield and a minor

species shifted further upfield ($\delta = 8.61$ and 5.86 ; cf. $\delta = 8.47$ for **14**). Based on the boron NMR data, we assigned the major species as the adduct. After 24 h, the imine had been completely consumed, only the adduct and the second species were present in approximately a 1:1 ratio. After 60 h, only the second species was present, generated in very high yield (>90%). Interestingly, this *in situ* ^1H NMR experiment showed that the conversion to the second product occurred at a rate competitive with imine coordination, as signals for the imine, adduct, and second product could all be observed at the same time.

Crystals for an X-ray diffraction study were obtained from a diethyl ether solution via vapor diffusion into hexanes and identified the product as the seven-membered BNC_5 heterocycle (**18**) resulting from the 1,2-insertion of the aldimine into the borole ring that we had initially expected (**Figure 6a**). To determine if heating would expedite the reaction, a toluene solution of borole **1** and imine **14** was heated at 80°C for 24 h. In this case, the reaction turned pale yellow instead of colorless, and a different signal in the $^{11}\text{B}\{^1\text{H}\}$ NMR spectrum ($\delta = 36.6$; cf. **18**, $\delta = 41.8$) was observed. Removing the volatiles *in vacuo*, washing the solids with hexanes, and drying afforded an off-white powder in 68% yield. The singlet in the ^1H NMR spectrum arising from the proton on the α -carbon of the imine was shifted upfield from the ring-expanded product ($\delta = 4.78$ ppm; cf. **18**, $\delta = 5.86$). Puzzled by this different product, we grew crystals for an X-ray diffraction study from a diethyl ether solution via vapor diffusion into hexanes, revealing the product as a seven-membered BNC_5 boat-like heterocycle (**19**) very similar to **18**, with the exception that the proton was now present on the carbon atom adjacent to boron instead of the

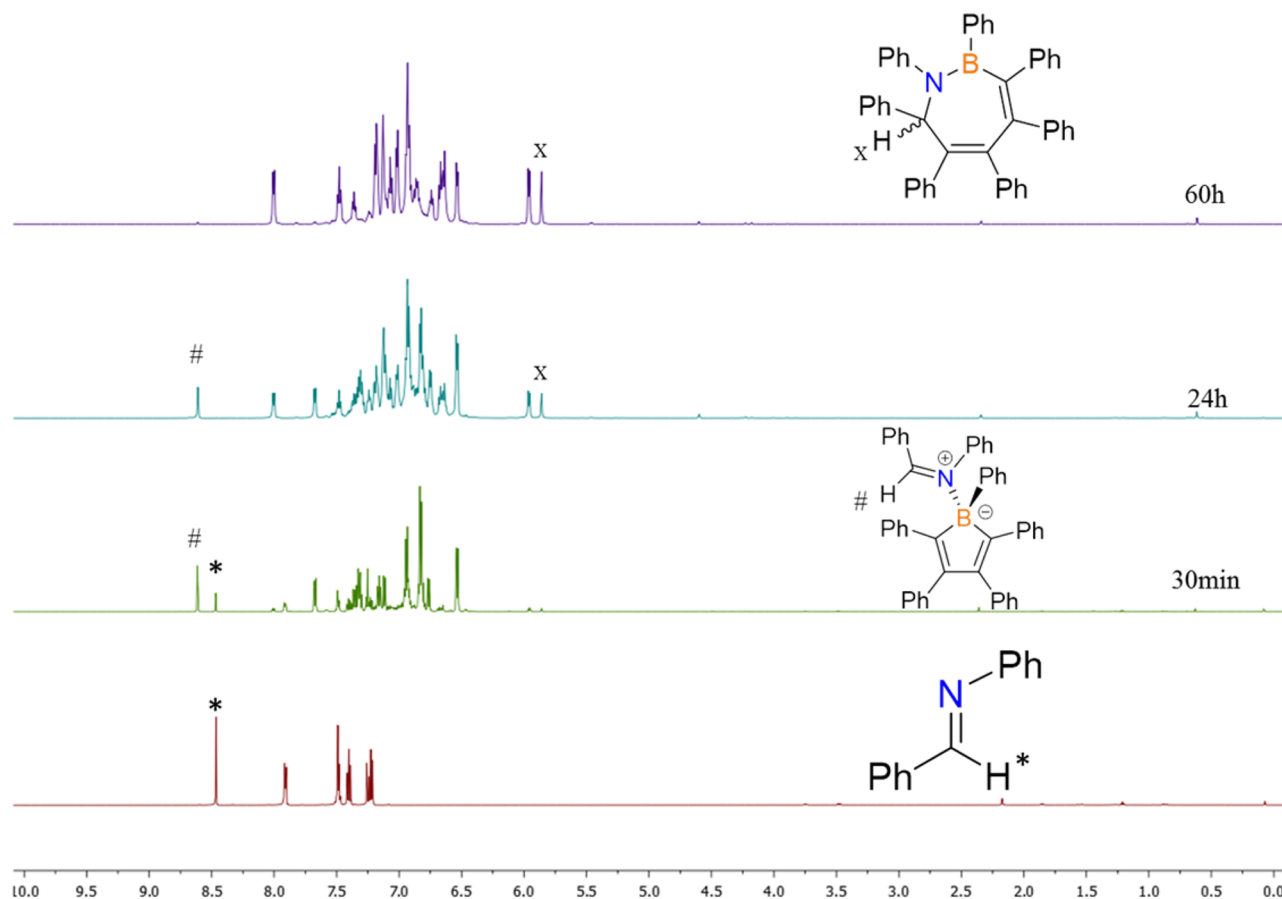


Figure 5. Stacked ^1H NMR plots displaying the reaction of borole **1** with imine **14** at room temperature in CDCl_3 .

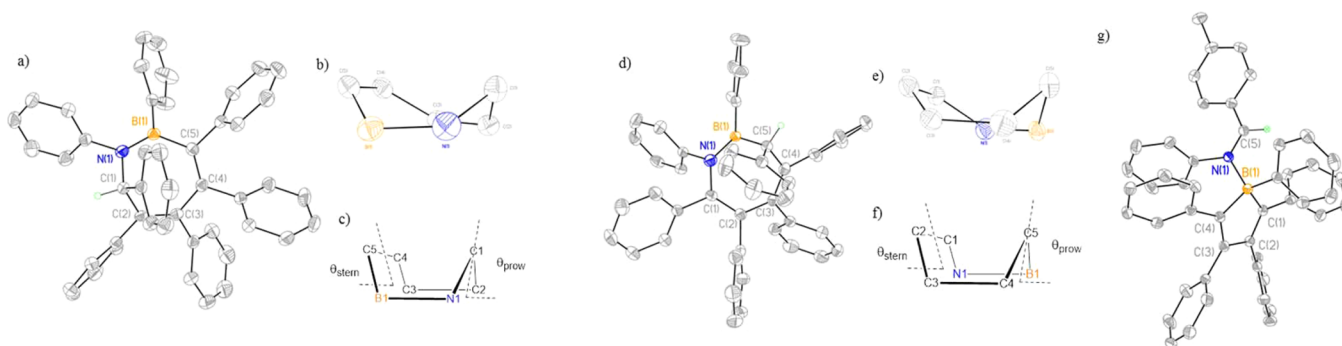
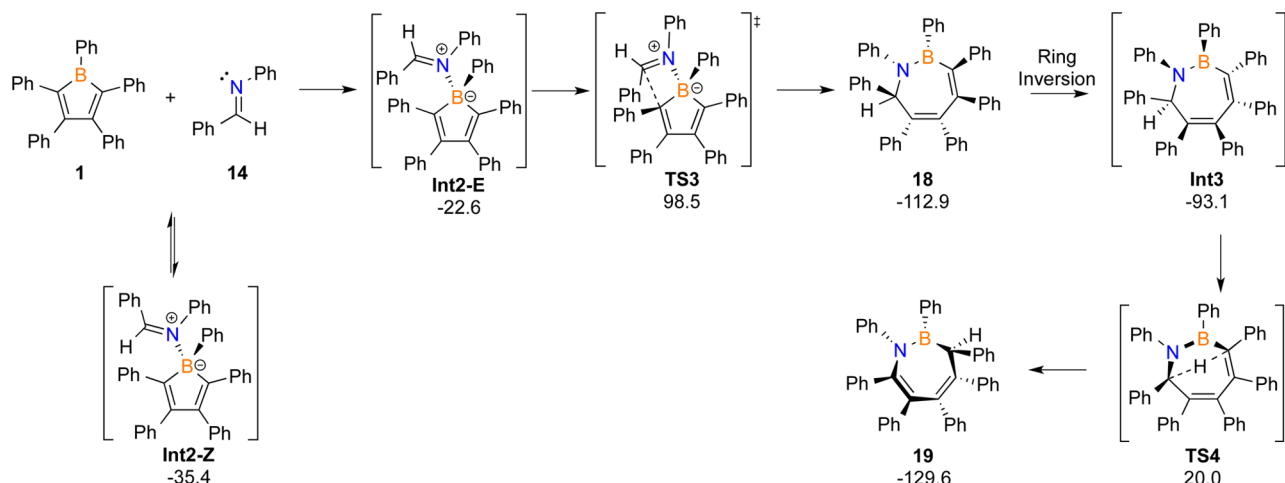


Figure 6. Solid-state structures of **18** (a) and **19** (d). Hydrogen atoms except on chiral centers are omitted for clarity, and ellipsoids are drawn at the 50% probability level. (a) Selected bond lengths (Å) and angles (deg) of **18**: B(1)–N(1) 1.392(2), N(1)–C(1) 1.4926(19), C(1)–C(2) 1.523(2), C(2)–C(3) 1.361(2), C(3)–C(4) 1.489(2), C(4)–C(5) 1.361(2), C(5)–B(1) 1.570(2), B(1)–C(61) 1.570(2), N(1)–B(1)–C(61) 121.86(14), N(1)–B(1)–C(5) 119.76(14). (b) View of the seven-membered ring in **18**. (c) Diagram illustrating the dihedral planes θ_{prow} [54.0(1)] and θ_{stem} [36.8(1)] defining the deviation of the ring from planarity into a boat-like conformation. (d) Selected bond lengths (Å) for **19**: B(1)–N(1) 1.402(3), N(1)–C(1) 1.438(2), C(1)–C(2) 1.359(3), C(2)–C(3) 1.462(2), C(3)–C(4) 1.383(3), C(4)–C(5) 1.540(3), C(5)–B(1) 1.567(3). (e) View of the seven-membered ring in **19**. (f) Diagram illustrating the dihedral planes θ_{prow} [58.2(2)] and θ_{stem} [35.3(1)] defining the deviation of the ring from planarity into a boat-like conformation. (g) Solid-state structure of **Int2CH₃-Z**. Hydrogen atoms (except on the aldimine carbon) and CH_2Cl_2 solvates are omitted for clarity. Ellipsoids are drawn at the 50% probability level. Selected bond lengths (Å) and angles (deg): B(1)–N(1) 1.623(2), B(1)–C(1) 1.634(2), B(1)–C(4) 1.632(2), N(1)–C(5) 1.2919(19), C(1)–C(2) 1.354(2), C(2)–C(3) 1.497(2), C(3)–C(4) 1.361(2), N(1)–B(1)–C(1) 107.00(12), N(1)–B(1)–C(4) 99.75(12), C(5)–N(1)–B(1) 123.16(13).

carbon adjacent to nitrogen (Figure 6d). Both **18** and **19** crystallized in centrosymmetric space groups containing both enantiomers in the unit cell, with the other enantiomer generated by symmetry.

With phenyl groups on every ring atom in **18**, it was difficult to determine if there was a rearrangement or a different

reaction or if the hydrogen had simply migrated. To probe this, we labeled the phenyl group on the α -carbon of the imine with a methyl group in the 4-position (**14CH₃**). Stirring a solution of borole **1** and imine **14CH₃** for 60 h at room temperature produced the analogous ring-expanded product (**18CH₃**) with the tolyl group and hydrogen atom bound to the carbon

Scheme 3. Theoretical Mechanistic Investigation of the Reaction of Imine 14 with 1^a

^aReaction energies (ΔG) in kJ/mol relative to 1 and 14.

adjacent to the nitrogen atom determined by X-ray crystallography (see [Supporting Information](#)). The shift for the diagnostic proton residing on the α -carbon formerly of the imine and the boron nucleus had essentially the same chemical shifts as the phenyl analogue 18 (18CH₃, ¹H δ = 5.87, ¹¹B{¹H} δ = 40.8; cf. 18, ¹H δ = 5.86, ¹¹B{¹H} δ = 41.8). While conducting these studies, the adduct was crystallized as the *Z*-conformer (Int2CH₃-Z, [Figure 6g](#)), indicating that *E* to *Z* isomerization occurred. The *E/Z* transformation of aldimines has been observed by Piers et al. in similar reactions with the strong Lewis acid tris(pentafluorophenyl)borane.¹⁸ In their studies, the *Z*-isomer minimized steric interactions and was thermodynamically favored.

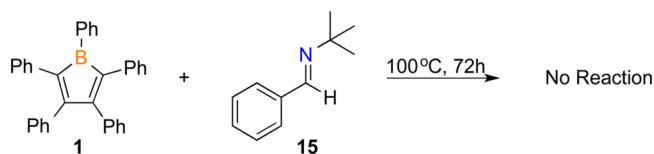
Thermolysis of 18CH₃ under the same conditions as 18 produced a species with a ¹¹B{¹H} NMR signal at 35.1 ppm and a singlet in the proton NMR spectrum at 4.76 ppm, in accord with those observed for 19 (¹¹B{¹H} δ = 36.6, ¹H δ = 4.78). An X-ray diffraction study revealed that the tolyl group was indeed still present on the carbon atom adjacent to the nitrogen and the hydrogen had moved to the carbon beside boron, confirming the identity as 19CH₃ (see [Supporting Information](#)). This result suggested that the hydrogen had migrated in both compounds to produce the complex with the proton on the carbon adjacent to boron.

An analysis of the relative thermodynamic energies of 1, 14, 18, and 19 using theoretical methods showed coordination of the imine to form the borole adduct (Int2, [Scheme 3](#)). A comparison of the relative energies of the two isomers (Int2-E and Int2-Z) shows that Int2-Z is calculated to be lower in energy than the *E*-isomer Int2-E (Int2-Z = -35.4 kJ/mol; cf. Int2-E = -22.6 kJ/mol), rationalizing the crystallization of Int2CH₃-Z. However, the orientation of the Ph and H substituents on the α -carbon of the adduct is critical for obtaining 18, specifically the H substituent pointing away from the borole in Int2-E. It is known that aldimines can isomerize and the reaction barrier is lower to proceed through Int2-E, with a calculated value for the ring expansion from Int2-E to 18 of 121.1 kJ/mol.⁵³ The transition barrier directly from Int2-Z to Int3 was located, but found to be approximately 10 kJ/mol higher in energy at 131.4 kJ/mol. Compound 19 is 16.7 kJ/mol lower in energy than 18, indicating that 18 is the kinetic product, while 19 is the thermodynamic product, which is

consistent with the experimental observations. Conversion of 18 to 19 is predicted to occur via a ring-flipping mechanism, although attempts to locate a transition state between 18 and the corresponding ring-flipped species Int3 were unsuccessful. However, the literature shows seven-membered heterocyclic rings have ring-flipping barriers in the range 40–60 kJ/mol.^{54–56} The species then has the proper orientation to undergo a [1,5]-hydride shift with a barrier of 113.1 kJ/mol to produce 19. Similar suprafacial sigmatropic [1,5]-hydride shifts have been observed in 1,3-cycloheptadienes that have comparable calculated barriers (115.1 kJ/mol).^{57,58}

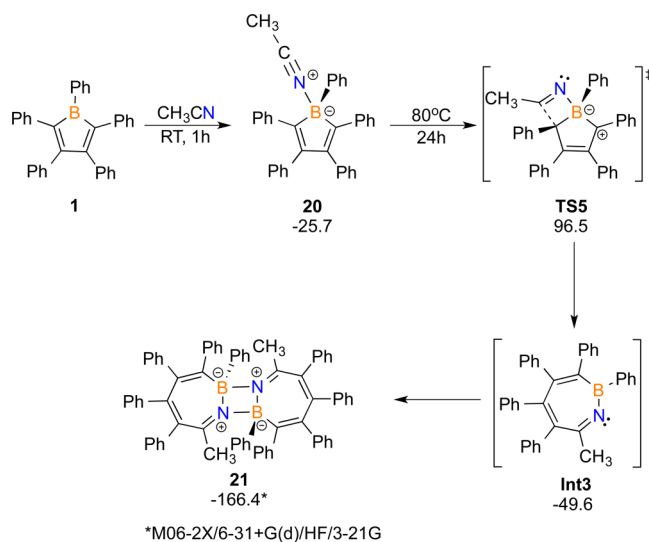
The reaction of the *N*-*tert*-butyl-substituted imine 15 with borole 1 showed no evidence of reaction by ¹H and ¹¹B{¹H} NMR spectroscopy or any color change from the blue borole, even after heating at 100 °C for 72 h ([Scheme 4](#)). The bulky

Scheme 4. Attempted Reaction of Imine 15 with 1



tert-butyl group on the nitrogen atom of 15 likely precludes any adduct formation, indicating that the coordination step is crucial for a ring expansion or an aryl C–H bond activation process. Theoretical calculations support that adduct formation of 15 with 1 is unfavorable by 13 kJ/mol.

To investigate triply bonded C–N systems, acetonitrile was reacted with borole 1 ([Scheme 5](#)). Adding one equivalent of acetonitrile to a solution of 1 in CH₂Cl₂ at room temperature resulted in the immediate color change from dark blue to yellow. Removing the volatiles *in vacuo* and obtaining a ¹H NMR spectrum of the redissolved solids in CDCl₃ displayed a single product with a diagnostic singlet for the methyl group of the nitrile integrating to three with respect to the 25 aryl protons shifted upfield in comparison to the free nitrile (δ = 1.48; cf. δ = 2.10). A single ¹¹B{¹H} NMR spectroscopic resonance was observed in the range of a four-coordinate boron species at -1 ppm. The FT-IR spectrum showed a diagnostic band for the C \equiv N stretching mode at 2342 cm⁻¹, similar to values observed for other acetonitrile-borane adducts.^{59–61} A

Scheme 5. Reaction of **1** with Acetonitrile^a

^aReaction energies (ΔG) are in kJ/mol relative to **1** and CH_3CN .

single-crystal X-ray diffraction study confirmed the product to be the adduct **20** (Figure 7a). The nitrile remains linear [$\text{N}(1)-\text{C}(6)-\text{C}(7) = 178.8(2)^\circ$] and is also bonded in a linear orientation to the boron center [$\text{B}(1)-\text{N}(1)-\text{C}(6) = 175.75(18)^\circ$]. The B–N and C–N bond distances of 1.573(2) and 1.132(2) Å, respectively, are comparable to those reported in other boron-acetonitrile adducts and consistent with the retention of the carbon–nitrogen triple bond.^{59–64} The adduct is relatively weak, with a calculated ΔG of -25.7 kJ/mol for the reaction between the borole and acetonitrile.

To investigate if adduct **20** would undergo a ring expansion to a seven-membered boracycle, a toluene solution of **20** was heated at 80°C for 24 h. The color of the solution remained yellow, but the $^{11}\text{B}\{^1\text{H}\}$ NMR showed a single peak at $\delta = 5.3$ and the disappearance of the peak corresponding to **20** at -1.1 ppm, indicating conversion of the borole- CH_3CN adduct to a new tetracoordinated boron species. An X-ray diffraction study indicated that adduct **20** went through a 1,2-insertion reaction

to form a seven-membered BNC_5 ring, which subsequently dimerized via intermolecular boron–nitrogen coordination to give the four-coordinate species **21** (Figure 7b). The molecule crystallizes in the $P\bar{1}$ space group with the monomer in the asymmetric unit, and the other half of the dimer is generated by symmetry (**21** crystallizes with three independent molecules in the asymmetric unit; only one representative molecule is shown and discussed). The $\text{N}(1)-\text{B}(1)-\text{N}(1\text{A})$ and $\text{C}(1)-\text{B}(1)-\text{N}(1)$ angles are $86.10(19)^\circ$ and $105.9(2)^\circ$, respectively, indicating a distorted tetrahedral environment about boron as expected for a B–N dimeric system. The two phenyl groups on the boron centers are oriented *trans* to one another. There is distinct bond length alternation within the ring, with C1–C2, C3–C4, and C6–N1 exhibiting double-bond character.

Theoretical calculations determined a ΔG for the formation of the seven-membered monomeric intermediate (Int3) from adduct **20** to be -23.9 kJ/mol with a transition state with a barrier of 122.2 kJ/mol relative to **20** (Scheme 5). Formation of the dimer was calculated to be favorable by -116.8 kJ/mol, justifying the resilience of the dimer in solution.

The *tert*-butylisocyanide/borole adduct **22** was analogously prepared by the treatment of borole **1** with $t\text{BuN}\equiv\text{C}$ in toluene (Scheme 6). The adduct exhibited a tetracoordinated $^{11}\text{B}\{^1\text{H}\}$ NMR chemical shift of $\delta = -12.1$ and was isolated in 96% yield. The FT-IR $\nu_{\text{N}\equiv\text{C}}$ band is shifted substantially to higher wavenumbers from the free isonitrile ($\nu_{\text{N}\equiv\text{C}} = 2251\text{ cm}^{-1}$; cf. 2140 cm^{-1}).^{59,65–67} Single crystals were obtained by vapor diffusion of diethyl ether into a toluene solution of **22** (Figure 8). Analogous to the acetonitrile adduct, the boron center sits in a slightly distorted tetrahedral environment. The *tert*-butyl group of the isocyanide is oriented slightly over one of the borole phenyl rings, likely causing a bending of the $\text{N}(1)-\text{C}(6)-\text{B}(1)$ angle to $169.7(2)^\circ$. The $\text{N}\equiv\text{C}$ bond length of 1.147(3) Å in adduct **22** is consistent with the retention of the triple bond. The formation of adduct **22** from *tert*-butyl isocyanide and borole **1** was calculated to be favorable by 68.7 kJ/mol. This value is much higher than the acetonitrile adduct (25.7 kJ/mol), accentuating the stronger sigma donation of the isocyanide ligand.

Heating a toluene solution of **22** at 80°C for 24 h resulted in a $^{11}\text{B}\{^1\text{H}\}$ NMR spectrum showing only one broad resonance

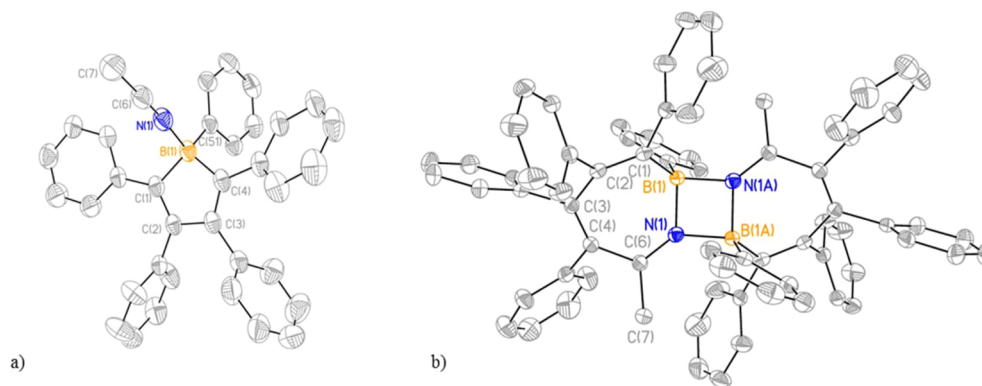
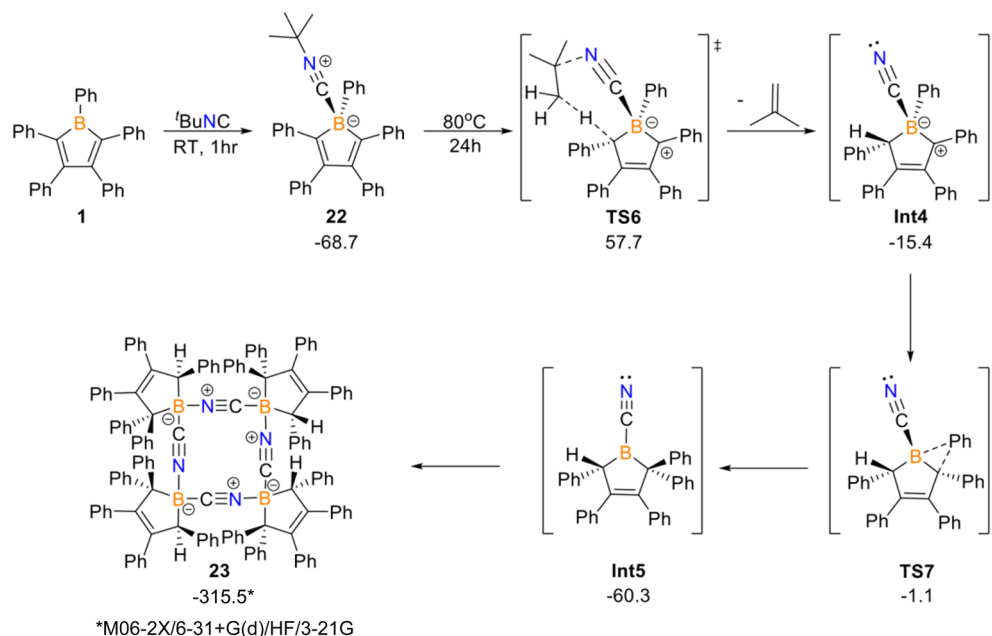


Figure 7. Solid-state structures of **20** (a) and **21** (b). Hydrogen atoms are omitted for clarity, and ellipsoids are drawn at the 50% probability level. Selected bond lengths (Å) and angles (deg) for **20**: B(1)–N(1) 1.573(2), B(1)–C(1) 1.620(3), B(1)–C(4) 1.613(3), B(1)–C(51) 1.613(3), N(1)–C(6) 1.132(2), C(1)–C(2) 1.357(3), C(2)–C(3) 1.489(2), C(3)–C(4) 1.353(2), C(6)–C(7) 1.451(3), N(1)–B(1)–C(51) 109.51(15), N(1)–B(1)–C(1) 109.73(14), B(1)–N(1)–C(6) 175.75(18), N(1)–C(6)–C(7) 178.8(2); for **21**: N(1)–B(1) 1.589(4), N(1)–C(6) 1.275(4), B(1)–C(1) 1.633(4), C(1)–C(2) 1.350(4), C(2)–C(3) 1.504(4), C(3)–C(4) 1.355(4), C(4)–C(6) 1.493(4), N(1)–B(1)–N(1A) 86.10(19), C(1)–B(1)–N(1) 105.9(2).

Scheme 6. Reaction of Pentaphenylborole with *tert*-Butyl Isocyanate^a

^aReaction energies (ΔG) are in kJ/mol relative to **1** and *t*BuNC.

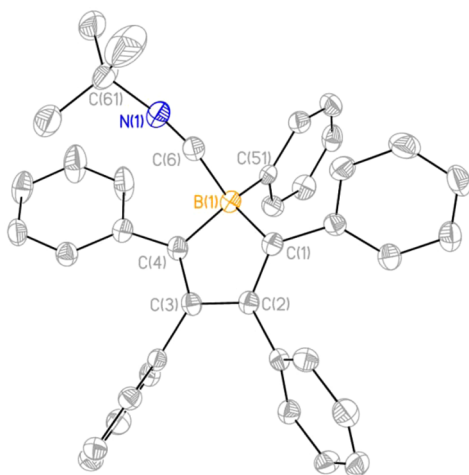


Figure 8. Solid-state structure of **22**. Hydrogen atoms were omitted for clarity, and ellipsoids are drawn at the 50% probability level. Selected bond lengths (Å) and angles (deg): B(1)–C(6) 1.593(4), B(1)–C(1) 1.613(3), B(1)–C(4) 1.617(3), B(1)–C(51) 1.622(3), N(1)–C(6) 1.147(3), C(1)–C(2) 1.358(3), C(2)–C(3) 1.494(3), C(3)–C(4) 1.365(3), N(1)–C(61) 1.468(3), C(6)–B(1)–C(51) 111.25(18), C(1)–B(1)–C(6) 112.8(2), N(1)–C(6)–B(1) 169.7(2).

at $\delta = -13$. Although the crude ^1H NMR spectrum indicated the product as a mixture, we were able to crystallize one species via vapor diffusion of pentane into a toluene solution. An X-ray diffraction study showed the solid-state structure to be the tetramer of five-membered boron rings bridged by cyano groups of **23**. A proton and a phenyl group were introduced on the carbon atoms adjacent to boron. The phenyl group from boron had moved to the carbon atom, and the proton could have originated from the lost *tert*-butyl group perhaps through the loss of isobutylene. An *in situ* ^1H NMR experiment conducted in a tube equipped with a Young's tap indeed displayed signals consistent with isobutylene (Supporting Information).

In this case, we had expected the electrophilic center of the Lewis base to be the carbon center. Contrary to the imine and nitrile chemistry, a ring expansion would result in a 1,1-insertion to give a six-membered ring reminiscent of the insertion reactions observed for carbon monoxide, diphenylacetylene, and a bulky azide (**4**, **5**, and **12**, Figure 1). This six-membered product is calculated to be unfavorable with a ΔG of +49.0 kJ/mol from adduct **22**. A pathway to give the observed product via the loss of isobutylene occurs by methyl deprotonation by the α -carbon of the borole ring (**TS6**), forming a carbocationic intermediate featuring a cyanide on boron (**Int4**, Scheme 6). This process is unfavorable by 53.3 kJ/mol with a barrier of 126.4 kJ/mol, making this process the rate-determining step. From this point, migration of a phenyl group to the carbocation giving **Int5** is favorable by 44.9 kJ/mol, with only a small barrier of 14.1 kJ/mol. Finally the tetramerization of **Int5** is favorable by 255.2 kJ/mol (at the modest HF/3-21G level of theory for this very large system), thereby driving the overall reaction.

Although a fascinating transformation, we still wanted to determine if ring expansion reactivity was possible with an isocyanide. The 2,6-dimethylphenyl isocyanide-borole adduct **24** was analogously prepared in quantitative yield. However, no further reaction was observed by heating or irradiating solutions of the adduct. Benzyl isocyanide was also tested in a reaction with borole **1**. In this case, the adduct (**25**) could be observed spectroscopically, but rapidly decomposed to a dark oil. Redissolving the oil in CDCl_3 and obtaining a ^1H NMR spectrum revealed a complex mixture. It is uncertain exactly why the isocyanides do not undergo a ring expansion reaction. It is noteworthy that the polarization of the isocyanide differs significantly from the isomeric nitrile and has a closer resemblance to carbon monoxide that underwent a 1,1-insertion reaction with **1** to insert a single carbon atom rather than a 1,2-insertion; however as noted above this is calculated to be thermodynamically unfavorable in this particular case.

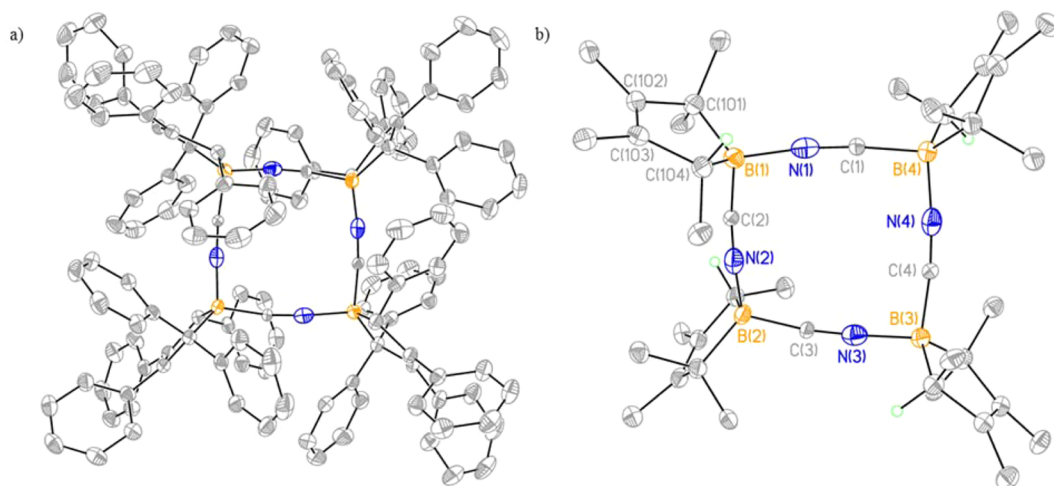


Figure 9. (a) Solid-state structure of (*S,R,S,R*)-**23**. Hydrogen atoms were omitted for clarity, and ellipsoids are drawn at the 50% probability level. (b) Tetramer structure of **23** showing chiral carbons in the boron five-membered ring. Phenyl groups were omitted for clarity. Selected bond lengths (Å) and angles (deg): C(1)–N(1) 1.153(2), B(1)–N(1) 1.588(3), B(1)–C(2) 1.576(3), B(1)–C(101) 1.673(3), C(101)–C(102) 1.545(3), C(102)–C(103) 1.346(3), C(103)–C(104) 1.525(3), C(104)–B(1) 1.633(3), N(1)–B(1)–C(2) 99.68(14), N(1)–B(1)–C(101) 115.93(15), C(101)–B(1)–C(104) 105.20(15).

CONCLUSION

In summary, we have reported the reactions of pentaphenylborole with unsaturated carbon–nitrogen molecules, namely, imines, nitriles, and isocyanides. We had anticipated that these species would form adducts that could readily be converted to the ring-expanded conjugated BN hybrid organic/inorganic heterocycles. Surprisingly, this outcome was not always observed. For an imine bearing two aryl groups on the α -carbon, the adduct could be isolated. Heating activated one of the *ortho* C–H bonds introducing the groups in a *syn* configuration at the 2- and 5-positions of the borole. The reaction with an imine bearing a hydrogen on the α -carbon atom resulted in the expected ring expansion occurring at room temperature from the coordination complex. Heating the reaction resulted in the migration of the hydride to the carbon adjacent to the boron center to form the thermodynamic product. The imine with a bulky *tert*-butyl group on nitrogen prevented any reaction from occurring. We attributed this to the bulk preventing coordination that is required for the C–H activation or ring expansion process to occur. The reaction of borole with acetonitrile cleanly produced the adduct that could be thermally converted to the seven-membered ring insertion product. The product dimerized through intermolecular B–N contacts due to the lack of bulk at boron and nitrogen. Isocyanides reacted with pentaphenylborole to produce adducts, but could not be converted into larger boracycles. One product could be isolated from heating the *tert*-butyl isocyanide adduct, revealing a cyano-bridged tetramer. These studies shed light on the reactivity of borole with 1,2-dipolar molecules. The results indicate that the ring expansion reaction is not universal and other interesting reactions can take place. The mechanistic studies provide insight into previous synthetic observations and assist in predicting future reactivity of antiaromatic boroles.

EXPERIMENTAL SECTION

General Considerations. All manipulations were performed under an inert atmosphere in a nitrogen-filled MBraun Unilab glovebox or using standard Schlenk techniques. Solvents were purchased from commercial sources as anhydrous grade, dried further

using a JC Meyer solvent system with dual columns packed with solvent-appropriate drying agents, and stored over molecular sieves. 2,6-Dimethylphenyl isocyanide and *tert*-butyl were purchased from Alfa Aesar and used as received. Benzyl isocyanide was purchased from TCI and used as received. Borole **1** and imines **13**–**15** were prepared via the literature procedures.^{4,68} Solvents for NMR spectroscopy were purchased from Cambridge Isotope Laboratories and dried by stirring over CaH₂ for 3 days, distilled, and stored over 4 Å molecular sieves. Multinuclear NMR spectra were recorded on Varian VNMRs 500 MHz or Bruker 360, 400, or 600 MHz spectrometers. FT-IR spectra were recorded on a Bruker Alpha ATR FT-IR spectrometer on the solid samples. High-resolution mass spectra (HRSM) were obtained on a Micromass Autospec Ultima. Single-crystal X-ray diffraction data were collected on a Bruker Apex II-CCD detector using Mo K α radiation ($\lambda = 0.71073$ Å).

Computational Methods. All calculations were carried out within Gaussian 09.⁶⁹ Geometries of all structures were optimized using the M06-2X⁷⁰ density functional theory (DFT) method. All structures were optimized with the 6-31+G(d) basis set.^{71,72} For larger systems (dimers and tetramers), geometry optimizations were carried out using the HF/3-21G level of theory with M06-2x/6-31+G(d) single-point energies in the interest of computational efficiency. Transition-state geometry optimizations employed the quadratic synchronous transit (QST) approach⁷³ and Gaussian-based algorithms for transition-state optimizations. Stationary points were characterized as minima or transition states by calculating the Hessian matrix analytically at the same level of theory. All structures labeled as minima exhibit no imaginary frequencies; transition states exhibit one imaginary frequency. Thermodynamic corrections were taken from these calculations (standard state of $T = 298.15$ K and $p = 1$ atm). Intrinsic reaction coordinate calculations were carried out to ensure transition states connected the appropriate local minima.

Single-point energies were calculated at the M06-2x and SCS-MP2⁷⁴ levels of theory inclusive of solvent effects with a polarizable continuum model (IEFPCM)^{75–77} with toluene solvent parameters using Truhlar's SMD solvation model.⁷⁸ Reported SCS-MP2 thermochemical data are SCS-MP2 electronic energies (inclusive of solvent effects) corrected by M06-2X/6-31+G(d) thermochemical corrections.

Synthesis of 16. At room temperature, a solution of *N*-benzyl-1,1-diphenylmethanimine (**13**) (36.6 mg, 0.135 mmol) in CH₂Cl₂ (1 mL) was added to a solution of borole **1** (60.0 mg, 0.135 mmol) in CH₂Cl₂ (1 mL), resulting in a color change from blue to red. After stirring for 1 h, the solvent was removed *in vacuo*, giving red solids. The solids

were washed with hexanes (2×0.3 mL) and dried *in vacuo* to give **16** as a red powder. Yield: 94.6 mg, 97%. Single crystals for X-ray diffraction studies were grown from a CH_2Cl_2 solution of **16** by vapor diffusion into hexanes. Mp = 148–149 °C; ^1H NMR (600 MHz, CDCl_3) δ 7.73–7.71 (m, 4H, C_6H_5), 7.56–7.51 (m, 1H, C_6H_5), 7.40 (t, J = 7.7 Hz, 4H, C_6H_5), 7.32–7.05 (m, 9H, C_6H_5), 7.04–6.80 (m, 19H, C_6H_5), 6.75–6.65 (m, 3H, C_6H_5), 5.32 (s, 2H, CH_2); $^{13}\text{C}\{^1\text{H}\}$ NMR (151 MHz, CDCl_3) δ 143.65, 140.07, 133.66 (br), 130.61 (br), 130.07 (br), 128.64, 128.11 (br), 127.67 (br), 127.43, 127.20 (br), 126.97, 126.92, 126.76, 126.36 (br), 125.15, 124.15; $^{11}\text{B}\{^1\text{H}\}$ NMR (193 MHz, CDCl_3) δ 6.0; FT-IR (cm^{-1} (ranked intensity)) 3055(2), 2043(12), 1948(15), 1597(4), 1491(3), 1443(5), 1316(7), 1075(13), 1028(6), 916(14), 768(9), 735(10), 696(1), 533(11), 420(8); HRMS chemical ionization (CI) calcd for $\text{C}_{54}\text{H}_{42}\text{BN} [\text{M}]^+$ 715.3410; found 715.3423.

Synthesis of 17. A toluene solution of **16** (50.0 mg, 0.070 mmol, 2 mL) was heated at 80 °C for 24 h. The volatiles were removed *in vacuo*, affording a pale yellow powder. The solids were washed with hexanes (2×0.3 mL) and dried *in vacuo* to give **17** as a pale yellow powder. Yield: 36.2 mg, 72% (estimated purity by ^1H NMR 94%). Single crystals for X-ray diffraction studies were grown from a CH_2Cl_2 solution of **17** by vapor diffusion into hexanes. Mp = 152–153 °C; ^1H NMR (600 MHz, CDCl_3) δ 8.44 (d, J = 7.8 Hz, 1H, aryl), 7.70 (d, J = 7.6 Hz, 1H, aryl), 7.57 (t, J = 7.6 Hz, 1H, aryl), 7.42–7.38 (m, 3H, aryl), 7.24–7.10 (m, 9H, aryl), 7.08–6.85 (m, 16H, aryl), 6.81–6.68 (m, 4H, aryl), 6.51 (t, J = 7.6 Hz, 1H, aryl), 6.39 (br, 1H, CH_2), 5.77 (d, J = 8.1 Hz, 1H, aryl), 5.31 (d, J = 16.1 Hz, 1H, aryl), 5.13 (d, J = 16.1 Hz, 1H, aryl), 5.02 (br, 1H, CH_2), 4.53 (s, 1H, CH); $^{13}\text{C}\{^1\text{H}\}$ NMR (151 MHz, CDCl_3) δ 177.13, 150.05, 149.18, 148.58, 146.75, 146.31, 141.63, 138.57, 137.31, 136.88, 134.94, 134.36, 133.25, 133.19, 132.38, 130.72, 130.44, 130.22, 130.14, 129.96, 129.86, 129.40, 128.75, 128.55, 128.12, 127.95, 127.80, 127.77, 127.72, 127.37, 127.19, 127.03, 126.78, 126.12, 126.01, 125.98, 125.89, 124.82, 124.78, 124.04, 123.13, 62.94, 59.64, 49.98; $^{11}\text{B}\{^1\text{H}\}$ NMR (193 MHz, CDCl_3) δ 4.7; FT-IR (cm^{-1} (ranked intensity)) 3052(3), 1595(2), 1557(8), 1492(4), 1442(7), 1339(5), 1156(10), 1060(15), 1029(9), 1000(14), 757(13), 699(1), 559(6), 541(11), 414(12); HRMS CI calcd for $\text{C}_{54}\text{H}_{42}\text{BN} [\text{M}]^+$ 715.3410; found 715.3417.

Synthesis of 18. At room temperature, a solution of (*E*)-*N*,1-diphenylmethanimine (**14**) (24.5 mg, 0.135 mmol) in CH_2Cl_2 (1 mL) was added to a solution of borole **1** (60.0 mg, 0.135 mmol) in CH_2Cl_2 (1 mL), resulting in a color change from blue to red. The red solution was stirred for 60 h, until the color disappeared completely. The solvent was removed *in vacuo*, and the solids were washed with hexanes (2×0.3 mL) and dried *in vacuo* to give **18** as an off-white powder. Yield: 77.6 mg, 92%. Single crystals for X-ray diffraction studies were grown from a diethyl ether solution of **18** by vapor diffusion into hexanes. Mp = 162–163 °C; ^1H NMR (600 MHz, CDCl_3) δ 8.00 (d, J = 8.2 Hz, 2H, C_6H_5), 7.49 (t, J = 7.7 Hz, 2H, C_6H_5), 7.38 (t, J = 7.4 Hz, 1H, C_6H_5), 7.23–7.16 (m, 4H, C_6H_5), 7.15–7.12 (m, 3H, C_6H_5), 7.10 (t, J = 7.4 Hz, 2H, C_6H_5), 7.07–6.99 (m, 3H, C_6H_5), 6.98–6.91 (m, 6H, C_6H_5), 6.91–6.85 (m, 2H, C_6H_5), 6.78–6.73 (m, 1H, C_6H_5), 6.71–6.62 (m, 5H, C_6H_5), 6.57–6.50 (m, 2H, C_6H_5), 6.06–5.90 (m, 2H, C_6H_5), 5.86 (s, 1H, CH); $^{13}\text{C}\{^1\text{H}\}$ NMR (151 MHz, CDCl_3) δ 150.19, 148.53, 144.00, 143.77, 143.13, 141.73, 141.44, 140.86, 140.83, 132.74, 131.29, 130.84, 130.75, 129.94, 128.80, 128.47, 127.98, 127.28, 127.11, 127.07, 127.01, 126.49, 126.43, 126.00, 125.83, 125.33, 125.22, 124.77, 74.09; $^{11}\text{B}\{^1\text{H}\}$ NMR (193 MHz, CDCl_3) δ 41.8 (br); FT-IR (cm^{-1} (ranked intensity)) 3054(3), 3022(14), 1597(4), 1490(2), 1441(10), 1235(6), 1179(12), 1134(13), 1078(9), 1029(7), 910(11), 762(8), 738(15), 697(1), 567(5); HRMS CI calcd. for $\text{C}_{47}\text{H}_{36}\text{BN} [\text{M}]^+$ 625.2941; found 625.2951.

Synthesis of 19. A toluene solution of **18** (30.0 mg, 0.048 mmol, 2 mL) was heated at 80 °C for 24 h, and the volatiles were removed *in vacuo*, affording a yellow powder. Recrystallization in CH_2Cl_2 at room temperature gave purified **19** as off-white solids. Yield: 20.4 mg, 68% (estimated purity by ^1H NMR 93%). Single crystals for X-ray diffraction studies were grown from a CH_2Cl_2 solution of **19** by vapor diffusion into hexanes. Mp = 195–196 °C; ^1H NMR (600 MHz, CDCl_3) δ 7.75 (d, J = 7.7 Hz, 2H, C_6H_5), 7.40 (t, J = 7.5 Hz, 2H,

C_6H_5), 7.29 (t, J = 7.5 Hz, 1H, C_6H_5), 7.21 (d, J = 6.3 Hz, 2H, C_6H_5), 7.16–7.08 (m, 5H, C_6H_5), 7.06–6.93 (m, 9H, C_6H_5), 6.89–6.83 (m, 4H, C_6H_5), 6.72–6.65 (m, 6H, C_6H_5), 6.57 (t, J = 7.6 Hz, 2H, C_6H_5), 5.82 (d, J = 7.6 Hz, 2H, C_6H_5), 4.78 (s, 1H, CH); $^{13}\text{C}\{^1\text{H}\}$ NMR (151 MHz, CDCl_3) δ 145.99, 143.84, 143.63, 141.26, 138.97, 138.43, 137.71, 137.49, 134.49, 132.34, 131.91, 131.90, 131.85, 129.83, 129.47, 128.83, 128.43, 127.89, 127.53, 127.28, 126.95, 126.52, 126.42, 126.21, 126.12, 126.01, 126.01, 125.26, 125.18, 48.71; $^{11}\text{B}\{^1\text{H}\}$ NMR (193 MHz, CDCl_3) δ 36.6; FT-IR (cm^{-1} (ranked intensity)) 3054(9), 1596(6), 1490(3), 1442(7), 1370(10), 1256(4), 1178(15), 1072(8), 906(2), 758(13), 728(12), 693(1), 649(11), 573(14), 532(5).

Synthesis of 20. At room temperature, acetonitrile (23.5 μL , 0.45 mmol) was added to a solution of borole **1** (200 mg, 0.45 mmol) in CH_2Cl_2 (3 mL), and the resulting yellow solution was stirred for 1 h. The solvent was removed *in vacuo*, giving a yellow solid. Yield: 216.2 mg, 99%. Single crystals for X-ray diffraction studies were grown from a CH_2Cl_2 solution of **20** by vapor diffusion into hexanes. Dp = 156 °C (turned dark red); ^1H NMR (500 MHz, CDCl_3) δ 7.53 (d, J = 7.6 Hz, 2H, C_6H_5), 7.32 (t, J = 7.6 Hz, 2H, C_6H_5), 7.25–7.17 (m, 1H, C_6H_5), 7.17–7.02 (m, 14H, C_6H_5), 7.03–6.93 (m, 6H, C_6H_5), 1.48 (s, 3H, CH_3); $^{13}\text{C}\{^1\text{H}\}$ NMR (151 MHz, CDCl_3) δ 150.83, 141.87, 139.69, 130.90, 130.18 (br), 128.82, 127.68, 127.45 (br), 127.42 (br), 127.30, 125.65, 125.35, 124.51, 1.70; $^{11}\text{B}\{^1\text{H}\}$ NMR (193 MHz, CDCl_3) δ –1.1; FT-IR (cm^{-1} (ranked intensity)) 3051(9), 3019(10), 2955(6), 2343(2), 1963(1), 1595(15), 1573(5), 1209(13), 1174(11), 1074(14), 1001(7), 979(8), 913(12), 841(4), 410(3).

Synthesis of 21. A toluene solution of **20** (60.0 mg, 0.124 mmol, 3 mL) was heated at 80 °C for 24 h. The volatiles were removed *in vacuo*, affording a yellow powder. Recrystallization in CH_2Cl_2 at room temperature gave **21** as a yellow solid, which was dried *in vacuo*. Yield: 40.7 mg, 68% (estimated purity by ^1H NMR 94%). Single crystals for X-ray diffraction studies were grown from a CH_2Cl_2 solution of **21** by vapor diffusion into hexanes. Mp: >240 °C; ^1H NMR (600 MHz, C_6D_6) δ 8.73 (d, J = 6.6 Hz, 4H, C_6H_5), 7.79 (t, J = 7.4 Hz, 4H, C_6H_5), 7.52 (t, J = 7.4 Hz, 2H, C_6H_5), 7.14–7.08 (m, 4H, C_6H_5), 7.02–6.92 (m, 9H, C_6H_5), 6.91–6.67 (m, 17H, C_6H_5), 6.68–6.57 (m, 5H, C_6H_5), 6.49–6.45 (m, 5H, C_6H_5), 0.91 (s, 6H, CH_3); $^{13}\text{C}\{^1\text{H}\}$ NMR (151 MHz, C_6D_6) δ 170.26, 148.70, 147.54, 145.32, 144.26, 143.69, 142.73, 142.57, 142.23, 141.01, 140.78, 140.59, 140.07, 139.29, 138.75, 138.04, 135.96, 132.00, 131.53, 131.19, 131.05, 131.02, 130.32, 129.97, 129.74, 129.58, 129.08, 128.85, 128.35, 127.23, 126.98, 126.95, 126.88, 126.84, 126.72, 126.51, 126.35, 126.25, 126.03, 125.57, 124.85, 23.00; $^{11}\text{B}\{^1\text{H}\}$ NMR (193 MHz, C_6D_6) δ 5.3; FT-IR (cm^{-1} (ranked intensity)) 3053(3), 3020(13), 1625(12), 1597(6), 1543(8), 1489(2), 1385(15), 1265(7), 1179(11), 1072(10), 1029(5), 965(14), 739(4), 697(1), 547(9); HRMS CI calcd for $\text{C}_{72}\text{H}_{56}\text{BN} [\text{M}]^+$ 970.4630; found 970.4638.

Synthesis of 22. At room temperature, *tert*-butylisocyanide (74.8 mg, 0.9 mmol) was added to a solution of borole **1** (400 mg, 0.9 mmol) in toluene (8 mL), and the resulting light green solution was stirred for 1 h. The solvent was removed *in vacuo*, giving a yellow solid. Yield: 454.8 mg, 96%. Single crystals for X-ray diffraction studies were grown from a CH_2Cl_2 solution of **22** by vapor diffusion into hexanes. Dp = 198 °C (turned black); ^1H NMR (360 MHz, CDCl_3) δ 7.39–7.31 (m, 2H, C_6H_5), 7.24–7.17 (m, 2H, C_6H_5), 7.14–7.06 (m, 7H, C_6H_5), 7.05–6.86 (m, 14H, C_6H_5), 1.47 (s, 9H, $\text{C}(\text{CH}_3)_3$); $^{13}\text{C}\{^1\text{H}\}$ NMR (91 MHz, CDCl_3) δ 151.66, 142.34, 139.90, 132.47, 130.41, 129.07, 127.68, 127.43, 127.39, 125.62, 125.25, 124.48, 59.40, 29.83; $^{11}\text{B}\{^1\text{H}\}$ NMR (116 MHz, CDCl_3) δ –12.1; FT-IR (cm^{-1} (ranked intensity)) 3057(13), 2251(2), 1591(7), 1484(6), 1439(15), 1182(9), 1027(10), 914(11), 792(14), 774(3), 734(5), 696(1), 563(12), 543(8), 520(4); HRMS CI calcd for $\text{C}_{39}\text{H}_{34}\text{BN} [\text{M}]^+$ 527.2784; found 527.2778.

Synthesis of 23. A toluene solution of **22** (50 mg, 0.095 mmol) was heated at 80 °C for 24 h. The volatiles were removed *in vacuo*, affording a yellow powder. Single crystals of **23** for X-ray diffraction studies were grown via vapor diffusion of pentane into a toluene solution. Despite numerous attempts we were unable to isolate a bulk sample of **23** (this is a minor product, see Supporting Information for crude ^1H NMR spectrum).

Synthesis of 24. At room temperature, a solution of 2,6-dimethylphenyl isocyanide (17.7 mg, 0.135 mmol) in CH_2Cl_2 (1 mL) was added to a solution of borole **1** (60.0 mg, 0.135 mmol) in CH_2Cl_2 (1 mL). The resulting red solution was stirred for 3 h. The solvent was removed *in vacuo*, giving a red solid. The solids were washed with hexanes (2×0.3 mL) and dried *in vacuo* to give **21** as a red powder. Yield: 73.9 mg, 95%; Dp = 168 °C (turned black); ^1H NMR (600 MHz, CDCl_3) δ 7.54 (d, J = 6.6 Hz, 2H, aryl), 7.35–7.27 (m, 3H, aryl), 7.24–7.09 (m, 9H, aryl), 7.08–6.94 (m, 14H, aryl), 2.27 (s, 6H, CH_3); $^{13}\text{C}\{^1\text{H}\}$ NMR (151 MHz, CDCl_3) δ 153.85, 152.45, 141.84, 139.90, 136.54, 132.75, 131.13, 130.31, 129.26, 128.53, 127.82, 127.52, 127.44, 125.72, 125.39, 124.67, 123.99, 18.41; $^{11}\text{B}\{^1\text{H}\}$ NMR (193 MHz, CDCl_3) δ –11.7; FT-IR (cm^{-1} (ranked intensity)) 3048(11), 2235(2), 1589(6), 1483(4), 1440(13), 1296(15), 1074(12), 1027(8), 908(10), 793(14), 773(5), 730(9), 694(1), 545(3), 490(7).

Synthesis of 25. At room temperature, a solution of benzyl isocyanide (17.7 mg, 0.135 mmol) in CH_2Cl_2 (1 mL) was added to a solution of borole **1** (60.0 mg, 0.135 mmol) in CH_2Cl_2 (1 mL). The resulting yellow solution was stirred for 1 min. The solvent was removed *in vacuo*, giving a yellow solid. The solids were washed with hexanes (2×0.3 mL) and dried *in vacuo* to give **17** as a yellow powder (decomposed rapidly in solution). Yield: 65.3 mg, 84% (estimated purity by ^1H NMR 91% likely due to decomposition); dp = 56 °C (turned black); ^1H NMR (400 MHz, CDCl_3) δ 7.39–7.31 (m, 5H, C_6H_5), 7.18–7.14 (m, 3H, C_6H_5), 7.13–7.09 (m, 2H, C_6H_5), 7.07–7.01 (m, 8H, C_6H_5), 6.98–6.91 (m, 9H, C_6H_5), 6.88–6.83 (m, 4H, C_6H_5), 4.89 (s, 2H, CH_2); $^{13}\text{C}\{^1\text{H}\}$ NMR (101 MHz, CDCl_3) δ 152.29, 142.04, 139.81, 132.60, 131.43, 130.37, 129.60, 129.51, 129.48, 129.42, 129.14, 128.85, 128.13, 128.03, 127.99, 127.74, 127.55, 127.51, 127.48, 127.23, 127.00, 126.94, 126.47, 126.42, 125.70, 125.37, 124.63, 47.97; $^{11}\text{B}\{^1\text{H}\}$ NMR (128 MHz, CDCl_3) δ –11.9; FT-IR (cm^{-1} (ranked intensity)) 3290(12), 3058(3), 2270(5), 2149(13), 1596(4), 1493(2), 1440(8), 1248(7), 1073(10), 1028(6), 911(15), 734(11), 697(1), 558(9), 429(14).

■ ASSOCIATED CONTENT

Supporting Information

The Supporting Information is available free of charge on the ACS Publications website at DOI: 10.1021/acs.inorgchem.5b01040.

Additional characterization details and spectra (PDF)
X-ray data (CIF)

■ AUTHOR INFORMATION

Corresponding Author

*E-mail: caleb_d_martin@baylor.edu.

Author Contributions

The manuscript was written through contributions of all authors. All authors have given approval to the final version of the manuscript.

Notes

The authors declare no competing financial interest.

■ ACKNOWLEDGMENTS

This work was generously supported by the Welch Foundation (Grant No. AA-1846) and Baylor University. La Trobe University, NCI-NF, and VPAC are acknowledged for generous grants of computing resources. This work is also supported by an ARC DECRA fellowship (JLD, DE130100186).

■ REFERENCES

- (1) Braunschweig, H.; Krummenacher, I.; Wahler, J. In *Advances in Organometallic Chemistry*; Hill, A. F., Fink, M. J., Eds.; Academic Press: San Diego, CA, 2013; Vol. 61, p 1.
- (2) Braunschweig, H.; Kupfer, T. *Chem. Commun.* **2011**, 47, 10903.
- (3) Braunschweig, H.; Fernández, I.; Frenking, G.; Kupfer, T. *Angew. Chem., Int. Ed.* **2008**, 47, 1951.
- (4) Eisch, J. J.; Hota, N. H.; Kozima, S. *J. Am. Chem. Soc.* **1969**, 91, 4575.
- (5) Herberich, G. E.; Buller, B.; Hessner, B.; Oschmann, W. *J. Organomet. Chem.* **1980**, 195, 253.
- (6) Eisch, J. J.; Galle, J. E.; Kozima, S. *J. Am. Chem. Soc.* **1986**, 108, 379.
- (7) Braunschweig, H.; Breher, F.; Chiu, C. W.; Gamon, D.; Nied, D.; Radacki, K. *Angew. Chem., Int. Ed.* **2010**, 49, 8975.
- (8) Braunschweig, H.; Chiu, C. W.; Wahler, J.; Radacki, K.; Kupfer, T. *Chem. - Eur. J.* **2010**, 16, 12229.
- (9) Bauer, J.; Braunschweig, H.; Hörl, C.; Radacki, K.; Wahler, J. *Chem. - Eur. J.* **2013**, 19, 13396.
- (10) Braunschweig, H.; Chiu, C. W.; Gamon, D.; Kaupp, M.; Krummenacher, I.; Kupfer, T.; Müller, R.; Radacki, K. *Chem. - Eur. J.* **2012**, 18, 11732.
- (11) Braunschweig, H.; Damme, A.; Gamon, D.; Kelch, H.; Krummenacher, I.; Kupfer, T.; Radacki, K. *Chem. - Eur. J.* **2012**, 18, 8430.
- (12) Braunschweig, H.; Dyakonov, V.; Jimenez-Halla, J. O. C.; Kraft, K.; Krummenacher, I.; Radacki, K.; Sperlich, A.; Wahler, J. *Angew. Chem., Int. Ed.* **2012**, 51, 2977.
- (13) So, C. W.; Watanabe, D.; Wakamiya, A.; Yamaguchi, S. *Organometallics* **2008**, 27, 3496.
- (14) Eisch, J. J.; Galle, J. E.; Shafii, B.; Rheingold, A. L. *Organometallics* **1990**, 9, 2342.
- (15) Eisch, J. J.; Galle, J. E. *J. Am. Chem. Soc.* **1975**, 97, 4436.
- (16) Ge, F.; Kehr, G.; Daniliuc, C. G.; Erker, G. *Organometallics* **2015**, 34, 229.
- (17) Fan, C.; Piers, W. E.; Parvez, M.; McDonald, R. *Organometallics* **2010**, 29, 5132.
- (18) Fan, C.; Mercier, L. G.; Piers, W. E.; Tuononen, H. M.; Parvez, M. *J. Am. Chem. Soc.* **2010**, 132, 9604.
- (19) Qu, Z. W.; Zhu, H. *J. Phys. Chem. C* **2013**, 117, 11989.
- (20) Braunschweig, H.; Damme, A.; Hörl, C.; Kupfer, T.; Wahler, J. *Organometallics* **2013**, 32, 6800.
- (21) Houghton, A. Y.; Karttunen, V. A.; Fan, C.; Piers, W. E.; Tuononen, H. M. *J. Am. Chem. Soc.* **2013**, 135, 941.
- (22) Braunschweig, H.; Kupfer, T. *Chem. Commun.* **2008**, 4487.
- (23) Braunschweig, H.; Chiu, C. W.; Radacki, K.; Kupfer, T. *Angew. Chem., Int. Ed.* **2010**, 49, 2041.
- (24) Ansorg, K.; Braunschweig, H.; Chiu, C. W.; Engels, B.; Gamon, D.; Hügel, M.; Kupfer, T.; Radacki, K. *Angew. Chem., Int. Ed.* **2011**, 50, 2833.
- (25) Braunschweig, H.; Chiu, C. W.; Damme, A.; Ferkinghoff, K.; Kraft, K.; Radacki, K.; Wahler, J. *Organometallics* **2011**, 30, 3210.
- (26) Braunschweig, H.; Damme, A.; Gamon, D.; Kupfer, T.; Radacki, K. *Inorg. Chem.* **2011**, 50, 4250.
- (27) Braunschweig, H.; Chiu, C. W.; Damme, A.; Engels, B.; Gamon, D.; Hörl, C.; Kupfer, T.; Krummenacher, I.; Radacki, K.; Walter, C. *Chem. - Eur. J.* **2012**, 18, 14292.
- (28) Braunschweig, H.; Damme, A.; Jimenez-Halla, J. O. C.; Hörl, C.; Krummenacher, I.; Kupfer, T.; Mailänder, L.; Radacki, K. *J. Am. Chem. Soc.* **2012**, 134, 20169.
- (29) Araki, T.; Fukazawa, A.; Yamaguchi, S. *Angew. Chem., Int. Ed.* **2012**, 51, 5484.
- (30) Braunschweig, H.; Chiu, C. W.; Gamon, D.; Gruß, K.; Hörl, C.; Kupfer, T.; Radacki, K.; Wahler, J. *Eur. J. Inorg. Chem.* **2013**, 2013, 1525.
- (31) Braunschweig, H.; Hörl, C.; Mailänder, L.; Radacki, K.; Wahler, J. *Chem. - Eur. J.* **2014**, 20, 9858.
- (32) Couchman, S. A.; Thompson, T. K.; Wilson, D. J. D.; Dutton, J. L.; Martin, C. D. *Chem. Commun.* **2014**, 50, 11724.
- (33) Huang, K.; Martin, C. D. *Inorg. Chem.* **2015**, 54, 1869.
- (34) Braunschweig, H.; Celik, M. A.; Hupp, F.; Krummenacher, I.; Mailänder, L. *Angew. Chem., Int. Ed.* **2015**, 54, 6347.

- (35) Fukazawa, A.; Dutton, J. L.; Fan, C.; Mercier, L. G.; Houghton, A. Y.; Wu, Q.; Piers, W. E.; Parvez, M. *Chem. Sci.* **2012**, *3*, 1814.
- (36) Steffen, A.; Ward, R. M.; Jones, W. D.; Marder, T. B. *Coord. Chem. Rev.* **2010**, *254*, 1950.
- (37) Muhammad, S.; Janjua, M. R.; Su, Z. *J. Phys. Chem. C* **2009**, *113*, 12551.
- (38) Collings, J. C.; Poon, S.-Y.; Le Droumaguet, C.; Charlot, M.; Katan, C.; Pålsson, L.-O.; Beeby, A.; Mosely, J. A.; Kaiser, H. M.; Kaufmann, D.; Wong, W.-Y.; Blanchard-Desce, M.; Marder, T. B. *Chem. - Eur. J.* **2009**, *15*, 198.
- (39) Li, H. Y.; Sundararaman, A.; Venkatasubbiah, K.; Jäkle, F. *J. Am. Chem. Soc.* **2007**, *129*, 5792.
- (40) Jäkle, F. *Chem. Rev.* **2010**, *110*, 3985.
- (41) Lorbach, A.; Hübner, A.; Wagner, M. *Dalton Trans.* **2012**, *41*, 6048.
- (42) Matsumi, N.; Chujo, Y. *Polym. J.* **2008**, *40*, 77.
- (43) Yin, X. D.; Chen, J. W.; Lalancette, R. A.; Marder, T. B.; Jäkle, F. *Angew. Chem., Int. Ed.* **2014**, *53*, 9761.
- (44) Caruso, A.; Tovar, J. D. *J. Org. Chem.* **2011**, *76*, 2227.
- (45) Caruso, A.; Siegler, M. A.; Tovar, J. D. *Angew. Chem., Int. Ed.* **2010**, *49*, 4213.
- (46) Levine, D. R.; Siegler, M. A.; Tovar, J. D. *J. Am. Chem. Soc.* **2014**, *136*, 7132.
- (47) Hudson, Z. M.; Wang, S. *Dalton Trans.* **2011**, *40*, 7805.
- (48) Campbell, P. G.; Marwitz, A. J. V.; Liu, S. Y. *Angew. Chem., Int. Ed.* **2012**, *51*, 6074.
- (49) Bodset, M. J. D.; Piers, W. E. *Can. J. Chem.* **2009**, *87*, 8.
- (50) Blackwell, J. M.; Piers, W. E.; Parvez, M.; McDonald, R. *Organometallics* **2002**, *21*, 1400.
- (51) The transition state must be higher in energy than the intermediate, but in this case the energies of the two species are within the accuracy of the method, resulting in a discrepancy where the intermediate is higher in energy. The intermediate has no negative vibration, and the transition state has a negative vibration associated with the transformation. The two species are connected as determined via an IRC calculation.
- (52) Ge, F.; Kehr, G.; Daniliuc, C. G.; Erker, G. *J. Am. Chem. Soc.* **2014**, *136*, 68.
- (53) The calculated barrier at TS3 is too high to be in good agreement with observed experimental conditions. Many possibilities were considered computationally, and the presented pathway is the set of calculations in best agreement with experimental observations, isolated intermediates, and literature precedent.
- (54) Fryer, R. I. In *Saturated Heterocyclic Chemistry: Vol. 4*; Parker, W., Ed.; The Royal Society of Chemistry: 1977; Vol. 4, p 268.
- (55) Hagen, H.; Reinoso, S.; Albrecht, M.; Boersma, J.; Spek, A. L.; van Koten, G. *J. Organomet. Chem.* **2000**, *608*, 27.
- (56) Fryer, R. I.; Walser, A. In *Chemistry of Heterocyclic Compounds*; John Wiley & Sons, Inc.: New York, 1991; p 209.
- (57) Baldwin, J. E.; Raghavan, A. S. *J. Org. Chem.* **2004**, *69*, 8128.
- (58) Hess, B. A.; Baldwin, J. E. *J. Org. Chem.* **2002**, *67*, 6025.
- (59) Jacobsen, H.; Berke, H.; Döring, S.; Kehr, G.; Erker, G.; Fröhlich, R.; Meyer, O. *Organometallics* **1999**, *18*, 1724.
- (60) Martin, E.; Hughes, D. L.; Hursthouse, M. B.; Male, L.; Lancaster, S. J. *Dalton Trans.* **2009**, 1593.
- (61) Metz, M. V.; Schwartz, D. J.; Stern, C. L.; Marks, T. J. *Organometallics* **2002**, *21*, 4159.
- (62) Chase, P. A.; Romero, P. E.; Piers, W. E.; Parvez, M.; Patrick, B. O. *Can. J. Chem.* **2005**, *83*, 2098.
- (63) Morgan, M. M.; Marwitz, A. J. V.; Piers, W. E.; Parvez, M. *Organometallics* **2013**, *32*, 317.
- (64) Bergquist, C.; Bridgewater, B. M.; Harlan, C. J.; Norton, J. R.; Friesner, R. A.; Parkin, G. *J. Am. Chem. Soc.* **2000**, *122*, 10581.
- (65) Ekkert, O.; Miera, G. G.; Wiegand, T.; Eckert, H.; Schirmer, B.; Petersen, J. L.; Daniliuc, C. G.; Fröhlich, R.; Grimme, S.; Kehr, G.; Erker, G. *Chem. Sci.* **2013**, *4*, 2657.
- (66) Feldmann, A.; Iida, A.; Fröhlich, R.; Yamaguchi, S.; Kehr, G.; Erker, G. *Organometallics* **2012**, *31*, 2445.
- (67) Bernsdorf, A.; Brand, H.; Hellmann, R.; Köckerling, M.; Schulz, A.; Villinger, A.; Voss, K. *J. Am. Chem. Soc.* **2009**, *131*, 8958.
- (68) Eisenberger, P.; Bailey, A. M.; Crudden, C. M. *J. Am. Chem. Soc.* **2012**, *134*, 17384.
- (69) Frisch, M. J.; Trucks, G. W.; Schlegel, H. B.; Scuseria, G. E.; Robb, M. A.; Cheeseman, J. R.; Scalmani, G.; Barone, V.; Mennucci, B.; Petersson, G. A.; Nakatsuji, H.; Caricato, M.; Li, X.; Hratchian, H. P.; Izmaylov, A. F.; Bloino, J.; Zheng, G.; Sonnenberg, J. L.; Hada, M.; Ehara, M.; Toyota, K.; Fukuda, R.; Hasegawa, J.; Ishida, M.; Nakajima, T.; Honda, Y.; Kitao, O.; Nakai, H.; Vreven, T.; Montgomery, J. A., Jr.; Peralta, J. E.; Ogliaro, F.; Bearpark, M.; Heyd, J. J.; Brothers, E.; Kudin, K. N.; Staroverov, V. N.; Keith, T.; Kobayashi, R.; Normand, J.; Raghavachari, K.; Rendell, A.; Burant, J. C.; Iyengar, S. S.; Tomasi, J.; Cossi, M.; Rega, N.; Millam, J. M.; Klene, M.; Knox, J. E.; Cross, J. B.; Bakken, V.; Adamo, C.; Jaramillo, J.; Gomperts, R.; Stratmann, R. E.; Yazyev, O.; Austin, A. J.; Cammi, R.; Pomelli, C.; Ochterski, J. W.; Martin, R. L.; Morokuma, K.; Zakrzewski, V. G.; Voth, G. A.; Salvador, P.; Dannenberg, J. J.; Dapprich, S.; Daniels, A. D.; Farkas, Ö.; Foresman, J. B.; Ortiz, J. V.; Cioslowski, J.; Fox, D. J. *Gaussian 09*, Revision D.01 ed.; Gaussian, Inc.: Wallingford, CT, 2009.
- (70) Zhao, Y.; Truhlar, D. G. *Theor. Chem. Acc.* **2008**, *120*, 215.
- (71) Hariharan, P. C.; Pople, J. A. *Theor. Chim. Acta* **1973**, *28*, 213.
- (72) Hehre, W. J.; Ditchfield, R.; Pople, J. A. *J. Chem. Phys.* **1972**, *56*, 2257.
- (73) Peng, C.; Ayala, P. Y.; Schlegel, H. B.; Frisch, M. J. *J. Comput. Chem.* **1996**, *17*, 49.
- (74) Gerenkamp, M.; Grimme, S. *Chem. Phys. Lett.* **2004**, *392*, 229.
- (75) Pomelli, C.; Tomasi, J.; Barone, V. *Theor. Chem. Acc.* **2001**, *105*, 446.
- (76) Tomasi, J.; Mennucci, B.; Cancès, E. *J. Mol. Struct.: THEOCHEM* **1999**, *464*, 211.
- (77) Cancès, E.; Mennucci, B.; Tomasi, J. *J. Chem. Phys.* **1997**, *107*, 3032.
- (78) Marenich, A. V.; Cramer, C. J.; Truhlar, D. G. *J. Phys. Chem. B* **2009**, *113*, 6378.